Kallio, K., Koponen, S., and Pulliainen, J., Feasibility of airborne imaging spectrometry for lake monitoring—a case study of spatial chlorophyll *a* distribution in two meso-eutrophic lakes. International Journal of Remote Sensing, vol. 24, no. 19, pp. 3771-3790, 2003.

INT. J. REMOTE SENSING, 2003, VOL. 24, NO. 19, 3771–3790

Taylor & Francis
Taylor & Francis Group

Feasibility of airborne imaging spectrometry for lake monitoring—a case study of spatial chlorophyll *a* distribution in two meso-eutrophic lakes

K. KALLIO

Finnish Environment Institute, P.O. Box 140, 00251 Helsinki, Finland;
e-mail: kari.y.kallio@vyh.fi

S. KOPONEN and J. PULLIAINEN

Laboratory of Space Technology, P.O. Box 3000, 02015 Helsinki University of Technology, Finland

(*Received 23 March 2001; in final form 8 July 2002*)

Abstract. The spatial distribution of the sum of chlorophyll *a* and phaeophytin *a* concentrations (chl-a) under light wind (0–2 $\mathrm{m\,s^{-1}}$) conditions was studied in two lakes with an AISA airborne imaging spectrometer. Chl-a was interpreted from AISA radiance data using an algorithm based on the near-infrared (700–710 nm) to red (660–665 nm) ratio. The results of Lake Lohjanjärvi demonstrate that the use of one monitoring station can result in over- or underestimation by 29–34% of the overall chl-a compared with an AISA-based estimation. In Lake Hiidenvesi, the AISA-based estimation for the mean chl-a with 95% confidence limits was $25.19 \pm 2.18\,\mu\mathrm{g\,l^{-1}}$. The use of AISA data together with chl-a measured at 15 *in situ* sampling stations decreased the relative standard error of the mean chl-a estimation from 20.2% to 4.0% compared with the use of 15 discrete samples only. The relative standard error of the mean chl-a using concentrations at the three routine monitoring stations was $15.9\,\mu\mathrm{g\,l^{-1}}$ (63.1%). The minimum and maximum chl-a in Lake Hiidenvesi were 2 and 101 $\mu\mathrm{g\,l^{-1}}$, 6 and 70 $\mu\mathrm{g\,l^{-1}}$ and 11 and 66 $\mu\mathrm{g\,l^{-1}}$, estimated using AISA data, data from 15 *in situ* stations and data from three routine *in situ* stations, respectively.

1. Introduction

The spatial distribution of phytoplankton, usually estimated indirectly by chlorophyll *a* concentration, is often patchy and the concentration can vary considerably in different parts of a lake. Phytoplankton distribution is dependent on hydrodynamics (horizontal movement and turbulent mixing) and ecological factors (e.g. phytoplankton properties, nutrients, grazers, light, temperature). Phytoplankton is usually transported by wind-induced currents to the downward end of a lake and accumulated there (Stauffer 1982, Reynolds 1994, Vergagen 1994, Webster and Hutchinson 1994). According to a literature study by Camarero and Catalan (1991), the main source of variation appears to be on a large scale (> 100 m). Particularly in small lakes, large-scale variability is constrained by the morphology and irregular shape

International Journal of Remote Sensing
ISSN 0143-1161 print/ISSN 1366-5901 online © 2003 Taylor & Francis Ltd
http://www.tandf.co.uk/journals
DOI: 10.1080/0143116021000023899

of a lake. The location of the nutrient input also affects the distribution of phytoplankton. According to Camarero and Catalan (1991), little is known about the small-scale variability in lakes and the factors that influence it. Schernewski *et al.* (2000) studied phytoplankton patchiness in a small, shallow lake and concluded that the most pronounced patches were linked with the presence of horizontal circulation eddies. Lewin (1992) pointed out that spatial patterns and processes in ecosystems may be different, depending on the resolution at which they are observed.

In an ideal case, monitoring of water bodies includes the determination of concentrations of water quality variables in three spatial dimensions, their variation in time and the processes that generate the spatial distribution and temporal variation (Van Stokkom *et al.* 1993, Fisher 1994). Phytoplankton monitoring carried out by environmental authorities is usually based on the determination of concentrations at one or a few fixed stations that are assumed to represent the overall distribution of phytoplankton in a lake. Vertical distribution of phytoplankton can be determined by taking water samples from several depths at one station, but reliable estimation of horizontal distribution would require water sampling from a high number of stations or transect measurements from a boat with a continuously functioning fluorometer. These ground-based methods are, however, time-consuming and results must be spatially interpolated to obtain contour maps of the phytoplankton distribution.

Remote sensing enables monitoring of the spatial distribution of phytoplankton in the surface water layer more effectively than ground-based methods. Data acquisition by remote sensing is fast, and large areas can be surveyed over a short period of time. In particular, airborne remote sensing has good spatial resolution of only a few metres, and spectral channels can be selected for optimal estimation of chlorophyll *a*. The satellite sensors meant for water quality estimations (e.g. SeaWiFS, MODIS) are designed for oceanic conditions (IOCCG 1998). In most cases they are not suitable for phytoplankton monitoring in lakes, due to the poor spatial resolution (typically from several hundred metres to 1000 m) and spectral configuration. In oceans, the estimation of phytoplankton by remote sensing is based on the spectral signature of chlorophyll *a* in the 400–550 nm region (Reilly *et al.* 1998). This wavelength region cannot be applied in lakes, mainly because absorption by coloured dissolved organic matter hides the spectral signature of chlorophyll *a* at these wavelengths. Instead, the interpretation of chlorophyll *a* from remote sensing data in lakes is usually based on the spectral region 660–715 nm (Dekker 1993, Gitelson *et al.* 1993, Kallio *et al.* 2001).

Estimation of chlorophyll *a* distribution in lakes by remote sensing techniques has included the use of airborne photography (Wrigley and Horne 1974, Horne and Wrigley 1975), airborne spectrometry (Dekker 1993, Jupp *et al.* 1994, Dekker *et al.* 1999, Heege and Fischer 2000, George and Malthus 2001, Östlund *et al.* 2001) and satellite sensors (Dekker and Peters 1993, Vos and Rijkeboer 2000, Giardino *et al.* 2001, Östlund *et al.* 2001). Results were usually reported in the form of concentration maps, but no quantitative analyses of the spatial distribution or quantitative comparison with information obtained by traditional sampling have been carried out.

The main objective of this study is to estimate the spatial distribution (horizontal distribution in the surface water layer) of the sum of chlorophyll *a* and phaeophytin *a* concentrations (collectively chl-a) by airborne remote sensing in two lakes. The distributions of chl-a are calculated from spatially high-resolution chl-a maps. The information obtained from the remote sensing measurements is compared with that from routine monitoring stations. This is done to demonstrate and analyse the quantitative spatial error characteristics of operational monitoring programmes based on discrete sampling.

2. Material and methods

2.1. *Description of the lakes and surveys*

The lakes in this study were Lohjanjärvi and Hiidenvesi, which were included in a series of remote sensing surveys carried out during 1996–1998 in 11 lakes in Finland. These surveys included airborne, satellite, optical and limnological measurements (Kallio *et al.* 2001, Koponen *et al.* 2001, Pulliainen *et al.* 2001).

Lakes Lohjanjärvi (60° 15′ N, 23° 55′ E) and Hiidenvesi (60° 23′ N, 24° 12′ E) are located in southern Finland, 50–70 km west of Helsinki. Both lakes consist of several sub-basins and include several islands and peninsulas. As a result, the water quality varies considerably with trophic status, ranging from mesotrophic to eutrophic (table 1). The main source of nutrient loading in both lakes is agriculture. The most eutrophic parts of these lakes suffer from algal blooms. In August 1998, swimming was temporarily prohibited at the public beaches in Lake Hiidenvesi, due to cyanobacterial blooms.

At Lake Lohjanjärvi, the spatial distribution of chl-a was studied in the Pappilanlahti and Aurlahti bays located in the eastern parts of the lake (figure 1(*a*)), where a large variation in water quality was expected. These bays are located in the most eutrophic parts of Lake Lohjanjärvi. About 70% of the total water flow comes from the Väänteenjoki and Pusulanjoki, agricultural rivers which discharge into Pappilanlahti bay through two small lakes. In addition, Aurlahti bay is loaded by paper mill and municipal wastewaters. Most of the shoreline in both bays is covered by a belt of helophytic macrophytes (with a maximum width of about 40 m), consisting mainly of common reed (*Phagmites australis*). The surveyed parts of the Pappilanlahti and Aurlahti bays are mostly 2–5 and 3–8 m deep, respectively. Both bays are routinely monitored in August at one fixed station (figure 1(*a*)).

About 30% of the area of Lake Hiidenvesi is deeper than 10 m, and most of the eutrophic eastern part consists of shallow nonstratified areas that function as a flow-through system (Tallberg *et al.* 1999). In many places, the shoreline is covered by a 10–30 m wide belt of helophytic macrophytes, particularly in the eastern part of Lake Hiidenvesi. The inflow consists of the Vihtijoki and Vanjoki rivers in the north-eastern and northern parts of the lake, respectively (figure 1(*b*)).

During the surveys, *in situ* water samples were taken during the aircraft overpass and within 3 h after the overpass. The number of sampling stations in Lakes

Table 1. Main characteristics of Lake Hiidenvesi and Lake Lohjanjärvi. The minimum and maximum values of water quality were based on the measurements made at the *in situ* sampling stations in the 0–0.4 m surface layer during the measurement campaigns (Lake Lohjanjärvi on 5–7 August 1996 and Lake Hiidenvesi on 11 August 1998).

Lake	Area km^2	Volume km^3	Mean depth m	Maximum depth m	Retention time d	Chl-a $\mu g\,l^{-1}$	TSS $mg\,l^{-1}$	Secchi m
Lohjanjärvi	94	1.16	12.3	50	750	6–44	2.3–10	0.9–2.4
Hiidenvesi	30	0.197	6.6	32	270	6–70	3–13	0.7–1.7

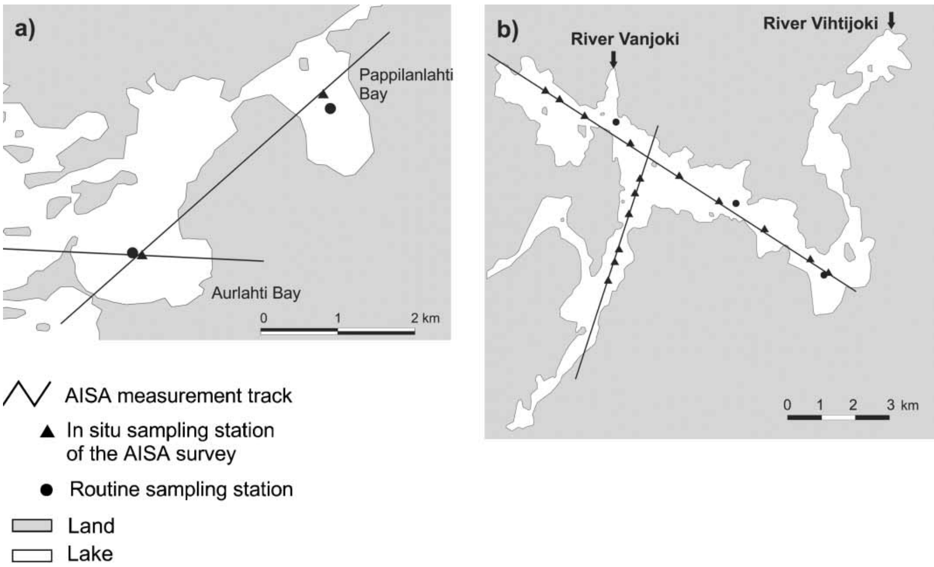

Figure 1. Location of *in situ* sampling stations used in the survey, location of routine sampling stations of the environment administration, and measurement tracks of the AISA airborne spectrometer at the Aurlahti and Pappilanlahti bays of Lake Lohjanjärvi (*a*) and at Lake Hiidenvesi (*b*).

Hiidenvesi and Lohjanjärvi were 15 and 5, respectively. All samples were taken from the surface layer at 0–0.4 m. At Lake Hiidenvesi, the measurements were carried out on 11 August 1998 and the 1140-m-wide image covered most of the lake area. In addition, data from August 1996 on Lake Hiidenvesi were used to confirm the chl-a interpretation algorithm. At Lake Lohjanjärvi the same measurements were repeated over three consecutive days on 5–7 August 1996, and the corresponding widths of the images were 380 and 610 m. During the surveys, the phytoplankton in both lakes was dominated by the cyanobacteria *Aphanizomenon spp.* Phytoplankton flakes were visible in the most eutrophic parts of both lakes, but no floating blooms were observed. Water temperature in the surface layer ranged from 17 to 21° C. Wind speed varied between 0 and $2\,m\,s^{-1}$ and the main wind direction was NW.

Methods of determination of limnological variables were as follows: the sum of chlorophyll *a* and phaeophytin *a* (ISO 10260) and total suspended solids (TSS, gravimetric determination of the matter removed by a Nuclepore polycarbonate $0.4\,\mu m$ filter). The ranges of water quality and surface temperature in both lakes are shown in table 1. Coloured dissolved organic matter (CDOM) was not measured in 1996 or 1998. In August 1997 the absorption coefficient of filtered water at 400 nm [$a_{CDOM}(400)$, spectrophotometric determination after filtration with a Nuclepore polycarbonate $0.4\,\mu m$ filter] was $3.8\,m^{-1}$ and $5.3\,m^{-1}$ in Aurlahti bay and Pappilanlahti bay, respectively. In Lake Hiidenvesi, $a_{CDOM}(400)$ ranged between $5.3\,m^{-1}$ and $6.0\,m^{-1}$ in August 1997.

2.2. *AISA airborne spectrometer*

The spectrometer used in the surveys was the AISA airborne imaging spectrometer (Mäkisara *et al.* 1993, Mäkisara 1998). The AISA is a pushbroom imager with a charge-coupled device (CCD) sensor matrix of 286×384 cells. The instantaneous field of view across the track is one milliradian, resulting in 1-m-wide pixels from an altitude of 1000 m. The integration time in the surveys ranged from 60 to 80 ms. The pixel length along the track was 4.5 m, using an integration time of 80 ms at an aircraft velocity of $55\,\mathrm{m\,s^{-1}}$. During the surveys, the flight altitudes were 1000, 1600 and 3000 m. The ground resolution varied from 1×4.5 m to 3×4.5 m. A pixel size of 2×2 m was selected for the geometrically and radiometrically corrected images. In addition, a video camera was installed on board the aircraft. The video images were used as an aid to identifying true water pixels near the shore in the AISA images.

The AISA was operated in full spatial resolution mode, in which images are stored for each selected spectral channel. The selected channels covered the 450–750 nm range almost continuously, with a channel width of 5–8 nm. The channel combinations of the various surveys differed slightly: the number of channels was 40 in August 1996 and 53 in August 1998. For comparison with the measured concentration, the AISA data were averaged from an area of 20×20 m at each *in situ* sampling station. Before each survey the AISA was radiometrically calibrated in the laboratory against a stable light source. The AISA was installed aboard a Short SC-7 Skyvan, the research aircraft of the Laboratory of Space Technology (Nikulainen *et al.* 1996). The coordinates of the sampling stations were determined in advance. The aircraft was equipped with a differential GPS navigation system that made it possible to overpass the sampling stations accurately.

3. Methods

3.1. *Interpretation of chl-a*

Several studies have shown that chl-a can best be estimated in lakes of a status ranging from oligotrophic to eutrophic by using the ratio of two channels at about 675 and 705 nm (Millie *et al.* 1992, Dekker 1993, Gitelson *et al.* 1993, Yacobi *et al.* 1995, Fraser 1998, Schalles *et al.* 1998).

In the present study, we wanted to demonstrate the potential usability of the Envisat MERIS satellite sensor launched in 2002. Therefore, the ratio $L_{700-710}/L_{660-665}$ that involves approximately the same channels as MERIS (Rast *et al.* 1999) was selected. Instead of the MERIS channel at 660–670 nm, the 660–665 nm region was used. An example of measured radiance spectra at Lake Lohjanjärvi is presented in figure 2. The peak at about 705 nm is due to absorption maximum of chl-a (at about 670 nm), absorption by pure water and backscattering by particles (e.g. Gitelson 1992, Gitelson *et al.* 2000).

Chl-a ($\hat{C}_{chl}$, $\mu\mathrm{g\,l^{-1}}$) was calculated from the AISA data by:

$$\hat{C}_{chl} = a\left(\frac{L_{700-710}}{L_{660-665}}\right) + b \qquad (1)$$

where a and b are empirical regression coefficients and $L_{700-710}$ and $L_{660-665}$ are upwelling radiances measured with AISA at 700–710 nm and 660–665 nm, respectively.

The empirical parameters in equation (1) were obtained by comparing the channel ratio $L_{700-710}/L_{660-665}$ with the measured chl-a at each observation station and using the least-squares method separately for both lakes. In Lake Lohjanjärvi, the AISA and *in situ* measurements from the entire lake were used to determine the empirical

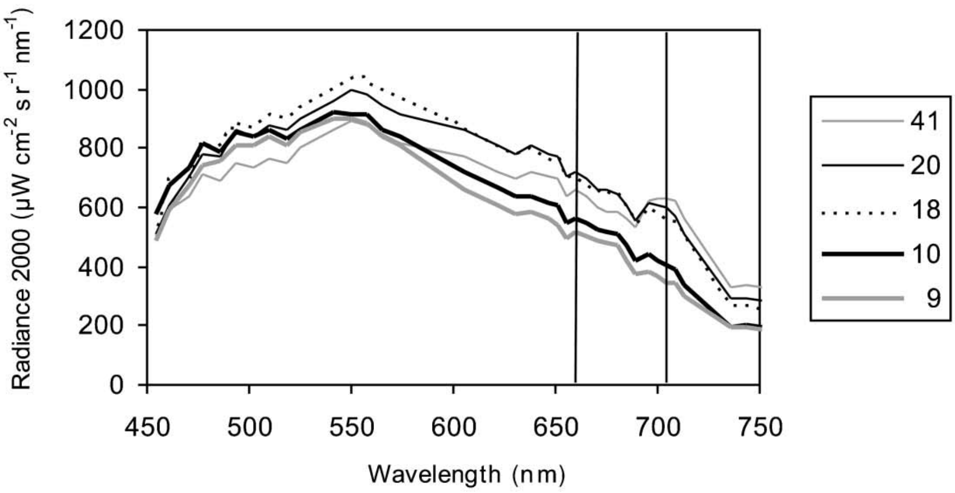

Figure 2. Measured AISA radiances at the five *in situ* stations with different chl-a (9–41 μg l^{-1}) at Lake Lohjanjärvi on 6 August 1996. Vertical lines indicate the channels (660–665 and 700–710 nm) used in the chl-a algorithm.

coefficients of the chl-a algorithm (five stations). The main accuracy characteristics determined for the algorithm were:

- R^2
- rms-error
- systematic error (bias)

rms-error is defined in the case of simple linear regression as

$$rmse = \sqrt{\frac{1}{N-2}\sum_{i=1}^{N}(C_{chl,i} - \hat{C}_{chl,i})^2} \tag{2}$$

where N is the total number of observations in the test dataset, $C_{chl,i}$ is the observed *in situ* chl-a and $\hat{C}_{chl,i}$ is the estimated chl-a.

Bias is defined as

$$bias = \frac{1}{N}\sum_{i=1}^{N}(C_{chl,i} - \hat{C}_{chl,i}) \tag{3}$$

Lake areas were separated from terrestrial areas in the AISA images using a digital land use and land cover mask (pixel size 25 m). The chl-a maps were constructed by applying the chl-a algorithm to each pixel of the AISA image of Lake Hiidenvesi and the eastern part of Lake Lohjanjärvi. Before the final statistical analyses of the chl-a maps, pixels with helophytic macrophytes and shadow on water were excluded. These pixels were identified based on the video camera images taken simultaneously with the AISA measurements. The statistical analyses of the chl-a on the maps included mean, minimum, maximum and median concentrations, and standard variation.

3.2. *Evaluation of the statistical accuracy of chl-a estimation*

With regard to operational lake water quality monitoring, it is essential to investigate the statistical accuracy characteristics of chl-a retrieval results. Here, we were especially interested in establishing how accurately the average chl-a of a lake (or a part of a lake) can be estimated from remote sensing data, or combined remote sensing and *in situ* data. The investigation of statistical accuracy characteristics also enables quantitative analysis of the benefits of remote sensing data, i.e. how large an accuracy improvement the use of remote sensing data can yield, compared with discrete water quality samples only.

Since the (random) error in chl-a estimates obtained by equation (1) is assumed to be normally distributed about the estimated regression line, the confidence interval for the estimated mean chl-a of the area under investigation (lake) is obtained as

$$\langle \hat{C}_{chl} \rangle \pm t_{\alpha/2} S \sqrt{\frac{1}{n} + \frac{(\langle X \rangle - \langle X_{ref} \rangle)^2}{S_{xx}}} \tag{4}$$

where $\langle \hat{C}_{chl} \rangle$ is the estimate based on remote sensing data for the mean chl-a in the study area, and $t_{\alpha/2}$ is a coefficient based on the T_{n-2} distribution. S is the rms-error for algorithm training data given by equation (2), and n is the number of samples in the training dataset. $\langle X \rangle$ is the mean of remotely sensed radiance ratios over the entire study area, and $\langle X_{ref} \rangle$ is the corresponding mean value for the algorithm training data. S_{xx} in equation (4) is given by

$$S_{xx} = \sum_{i=1}^{n} (x_{ref,i} - \langle X_{ref} \rangle)^2 \tag{5}$$

where $x_{ref,i}$ is the observed radiance ratio for training data point i.

In the present paper, the confidence intervals presented are the 95% bounds that indicate the limits within which the estimated mean locates with a probability of $\geqslant$95%.

Another statistical measure that is presented for mean chl-a estimates is the standard error (SE). This is presented for both *in situ* sampling and estimates based on remote sensing data. In the case of discrete *in situ* sampling, the SE of the estimated mean is

$$se_{\langle C_{chl} \rangle} = \frac{S_{\langle C_{chl,ref} \rangle}}{\sqrt{n}} = \sqrt{\frac{\sum_{i=1}^{n} (C_{chl,ref,\,i} - \langle C_{chl,ref} \rangle)^2}{n-1}} \frac{1}{\sqrt{n}} \tag{6}$$

Accordingly, the SE for the estimate based on remote sensing data for mean chl-a can be defined as

$$SE_{\langle C_{chl,\,AISA} \rangle} = S \sqrt{\frac{1}{n} + \frac{(\langle X \rangle - \langle X_{ref} \rangle)^2}{S_{xx}}} \tag{7}$$

The observed error for the discrete data was obtained as

$$E_{\langle C_{chl} \rangle} = |\langle C_{chl,ref} \rangle - \langle C_{chl,\,AISA} \rangle| \tag{8}$$

where $\langle C_{chl,AISA} \rangle$ is the mean of chl-a at discrete sampling stations and $\langle C_{chl,\,AISA} \rangle$ is the AISA-based estimate of the mean chl-a.

The SE (equations (6) and (7)) and E (equation (8)) can be directly compared to assess the quantitative improvement obtained by (1) the use of remote sensing data in addition to discrete sampling data and (2) the use of remote sensing data compared with the use of data from routine monitoring stations.

3.3. *Semivariogram analysis*

The quantitative spatial characteristics derived from a remote sensing dataset can be used to optimize the data sampling procedures from a remotely sensed image or to select an optimal pixel size for a remote sensing sensor. High spatial resolutions are expensive to purchase and laborious to process. For operational applications, the spatial resolution should not be finer than needed to fulfil the monitoring needs. One way to analyse these characteristics is to derive a semivariogram. The shape of a semivariogram can reveal some important aspects of the spatial dependency of the data. For example, the range of a semivariogram defines the distance at which semivariance (S^2) reaches maximum and above which the pixels are not related. This range can be considered to be the optimal pixel size.

The average semivariance ($\bar{S}^2$) of a data transect $z(x)$ with a lag h was here derived from the interpreted chl-a images using (Curran 1988):

$$\bar{S}^2 = \frac{1}{2m} \sum_{i=1}^{m} [C_{Chl,AISA}(l_i) - C_{Chl,AISA}(l_i + h)]^2 \qquad (9)$$

where m is the total length of a data transect (in pixels), $C_{chl,\ AISA}(l_i)$ is the chl-a in pixel l_i of the transect and h is the distance between pixels that are compared. The semivariogram is a graph in which $\bar{S}^2$ is presented as a function of lag (h). For the analyses, random transects (including long-track and cross-track) were extracted from the remotely sensed chl-a data. The h range varied between 1–40 and 1–2000 pixels, depending on the length of the transect.

4. Results

4.1. *Interpretation of chl-a*

The agreement between the calculated and observed chl-a was good in both lakes and R^2 was 0.98 and 0.96 for Lake Lohjanjärvi and Lake Hiidenvesi, respectively (figure 3(*a*), table 2). The empirical parameters of the chl-a algorithm differed only slightly between the two lakes. The results from Hiidenvesi in August 1996 (figure 3(*b*)) indicate that the relationship between the AISA radiance ratio (equation (1)) and chl-a was similar to that in August 1998. Comparison of the calculated chl-a (using the algorithm and empirical coefficients of August 1998) and the seven chl-a observations in 1996 in Lake Hiidenvesi yielded $R^2 = 0.98$, rmse $= 2.1\ \mu g\, l^{-1}$ and bias $= 2.0\ \mu g\, l^{-1}$.

4.2. *Chl-a maps*

The spatial variation of chl-a was considerable in both lakes. In Aurlahti bay, Lake Lohjanjärvi on 5 August 1996 most of the chl-a varied between 15 and 26 $\mu g\, l^{-1}$ (figure 4(*a*)). The concentrations were highest in the inshore areas and in the middle part of the upper section. The maximum concentration was 44 $\mu g\, l^{-1}$ (table 3). On 6 August the distribution of chl-a was more patchy than the day before (figure 4(*b*), table 3). In the centre of the surveyed area, the concentration was higher than 50 $\mu g\, l^{-1}$. This area continued to the east and west with chl-a of about 30 $\mu g\, l^{-1}$. A clear boundary is visible in the upper section of the map, with chl-a of 10–15 $\mu g\, l^{-1}$ in the north-western parts and 25 $\mu g\, l^{-1}$ in the central and south-eastern parts. The yellow-red grid in the eastern part of figure 4(*b*) is a complex of quays for small boats that was excluded from the statistical chl-a map analyses.

The chl-a images of Pappilanlahti bay (figure 5), on three consecutive days further indicate that the spatial distribution of chl-a at one location can vary with time. On

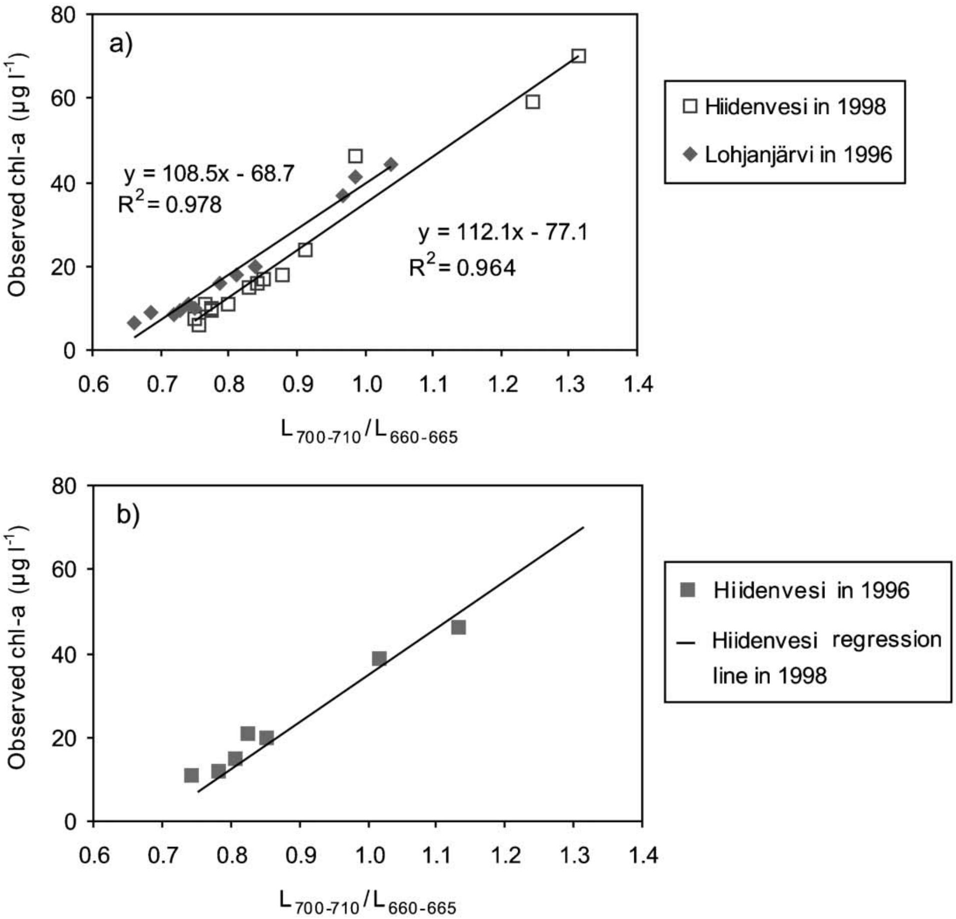

Figure 3. (*a*) Correlation between observed chl-a and the ratio of $L_{700-710}/L_{660-665}$ measured by the AISA at Lake Lohjanjärvi in 1996 and at Lake Hiidenvesi in 1998. (*b*) Correlation between observed chl-a and the ratio of $L_{700-710}/L_{660-665}$ measured by the AISA at Lake Hiidenvesi in 1996. In (*b*) the regression line of Lake Hiidenvesi in 1998 is also shown.

Table 2. Interpretation algorithms of chl-a in Lake Lohjanjärvi in 1996 and Lake Hiidenvesi in 1998.

Lake	Year	Algorithm	n	R^2	Rmse $\mu g l^{-1}$	rmse %
Lohjanjärvi	1996	Chl-a = 108.5*(L_{705}/L_{662}) − 68.7	12	0.978	2.13	11.1
Hiidenvesi	1998	Chl-a = 112.1*(L_{705}/L_{662}) − 77.1	15	0.964	3.87	17.3

5 and 6 August chl-a higher than $50\,\mu g l^{-1}$ were observed, while on 7 August no patchiness was observed. On 6 August chl-a formed an eddy-like spatial pattern.

According to the statistical analyses of the chl-a maps, the chl-a in Aurlahti bay varied between 8 and $55\,\mu g l^{-1}$ (figure 7(*a*), table 3). The concentration at the routine sampling station was less than the mean of chl-a on the map. In Pappilanlahti bay,

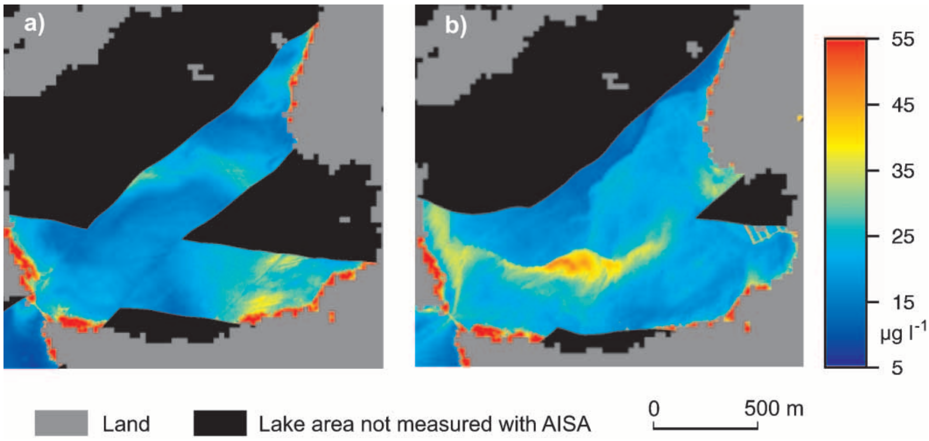

Figure 4. Chl-a interpreted from AISA airborne spectrometer data in Aurlahti bay, Lake Lohjanjärvi on 5 August 1996 (*a*) and 6 August 1996 (*b*).

the AISA-based estimation of the mean chl-a was almost the same on 5 and 6 August, but lower on 7 August (figure 7(*b*), table 3). At the routine sampling station the chl-a was similar to the AISA-based mean chl-a on 5 and 7 August, but on 6 August chl-a at the routine station was higher than the AISA-based mean chl-a. The maximum chl-a on the AISA maps of Pappilanlahti bay ranged from 50 to 76 $\mu g\,l^{-1}$ and the minimum from 16 to 22 $\mu g\,l^{-1}$ (table 3).

In the chl-a map of Lake Hiidenvesi, the colour scale indicating the chl-a levels was divided into eight classes (figure 6). To allow the separation of low concentrations in the western and central parts of Lake Hiidenvesi, narrow class limits were selected for the low concentrations. The chl-a between different parts of Lake Hiidenvesi varied considerably: in the most eutrophic south-eastern parts chl-a was more than 70 $\mu g\,l^{-1}$ in some places, while in the central parts chl-a varied between 10 and 40 $\mu g\,l^{-1}$ and in the north-western parts chl-a was less than 10 $\mu g\,l^{-1}$.

For further spatial analyses, Lake Hiidenvesi was divided into five rather homogeneous areas (figure 6). The variation of chl-a in areas 1 and 2 was small, while in areas 3, 4 and 5 the variation was wider (table 4, figure 8). The chl-a distribution of the whole lake (areas 1–5) was quite uniform in the high concentration region ($>30\,\mu g\,l^{-1}$) of the distribution diagram. The concentration region for chl-a less than 30 $\mu g\,l^{-1}$ was featured by the presence of two clear peaks: one at 8 $\mu g\,l^{-1}$ and the other at 19 $\mu g\,l^{-1}$. The chl-a at the routine sampling stations is located quite uniformly on the distribution diagram (figure 8(*a*)). However, the statistical characteristics of these three sampling stations (mean, minimum, maximum and standard deviation) are inadequate to describe the true spatial variation obtained with the AISA data (table 4).

The chl-a maps of Lake Hiidenvesi and Aurlahti bay are mosaics of two crossing images. As can be seen from the maps, there is no border (figures 4(*b*) and 6) or only a slight border (figure 4(*a*)) between the two images. This indicates that the chl-a interpretation algorithm is not sensitive to the change in measurement geometry (sun direction in relation to flight direction).

In the Lake Hiidenvesi data, the 95% confidence limits for AISA-based mean estimates as obtained by equation (4) were $25.19 \pm 2.18\,\mu g\,l^{-1}$. The number of *in situ*

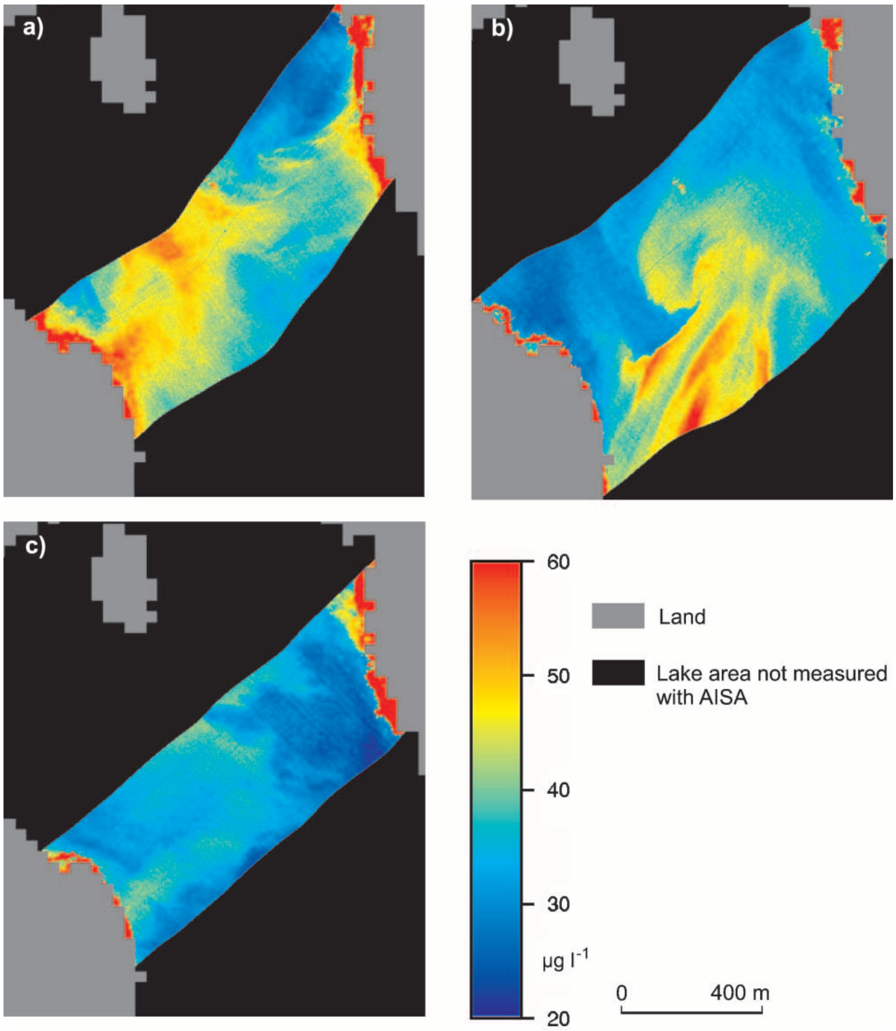

Figure 5. Chl-a interpreted from AISA airborne spectrometer data in Pappilanlahti bay, Lake Lohjanjärvi on 5(*a*), 6(*b*) and 7(*c*) August 1996.

reference chl-a observations in Lake Hiidenvesi was 15. The estimated mean value of this discrete data was

$$\langle \hat{X} \rangle = \langle X_{ref} \rangle = 22.41\ \mu g\, l^{-1}$$

According to equation (6) the standard error, $se_{\langle C_{chl} \rangle}$, for this estimate was 5.08 $\mu g\, l^{-1}$, which corresponds to a relative error of 20.2%, since the AISA-based estimate (25.19 $\mu g\, l^{-1}$) is considered to be an estimate of the true value. The standard error for AISA-based estimate was obtained by equation (7): $SE_{\langle C_{chl}, \mathrm{AISA} \rangle} = 1.00\ \mu g\, l^{-1}$, which yields a relative error of 4.0%.

The standard error, $se_{\langle C_{chl} \rangle}$, at the three routine sampling stations (obtained from the chl-a map, equation (6)) was $= 15.9\ \mu g\, l^{-1}$. This corresponds to a relative error of 63.1%. The observed error (equation (8)) for the chl-a at the 15 and three discrete

Table 3. Statistical characteristics of the chl-a maps of Lake Lohjanjärvi. The chl-a at the location of the routine sampling station on the map is also presented. STD = standard deviation. Observed error was calculated by equation (8).

	Aurlahti Bay		Pappilanlahti Bay		
	5 August 1996	6 August 1996	5 August 1996	6 August 1996	7 August 1996
Number of pixels	211 090	270 544	71 715	105 506	62 957
Area (km^2)	0.84	1.08	0.29	0.42	0.25
Mean chl-a ($\mu g\,l^{-1}$)	20.64	22.55	40.48	37.35	32.29
STD	4.74	5.81	6.68	6.82	4.12
Median chl-a ($\mu g\,l^{-1}$)	20	22	40	36	33
Minimum chl-a ($\mu g\,l^{-1}$)	10	8	21	22	16
Maximum chl-a ($\mu g\,l^{-1}$)	44	55	76	72	50
Chl-a at routine station ($\mu g\,l^{-1}$)	16	16	37	50	31
Observed error ($\mu g\,l^{-1}$)	4.6 (22.5%)	6.6 (29.1%)	3.5 (8.6%)	12.7 (33.9%)	1.3 (4.0%)

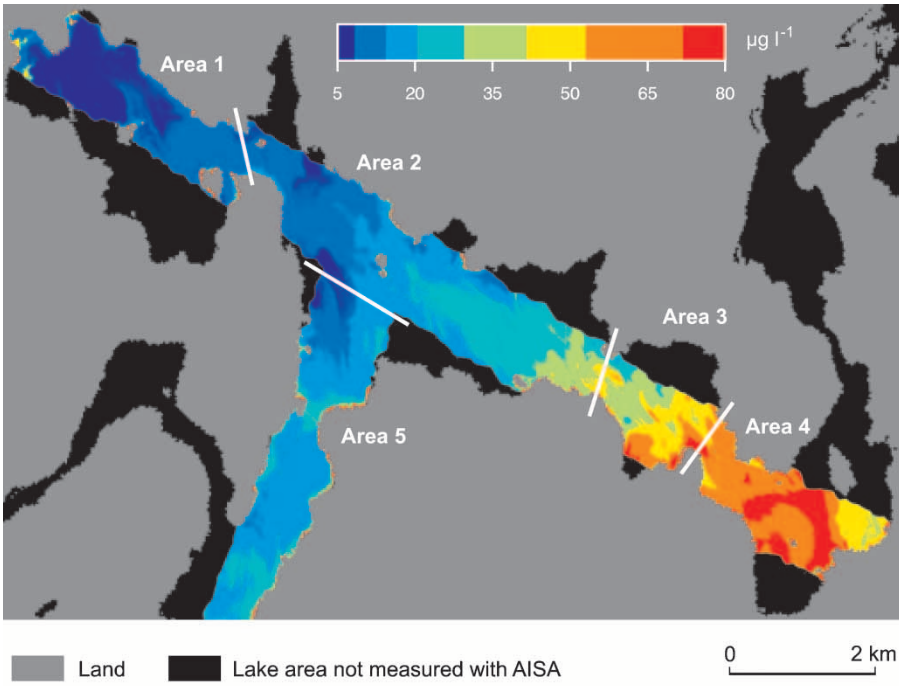

Figure 6. Chl-a interpreted from AISA airborne spectrometer data at Lake Hiidenvesi on 11 August 1998.

stations were 2.78 $\mu g\,l^{-1}$ and 11.8 $\mu g\,l^{-1}$, respectively. The calculated errors for Lake Hiidenvesi are summarized in tables 4 and 5.

The calculated semivariograms (equation (9)) were typically unbounded, since the correlation length grew with the transect length, so the range could not be determined. Even in Lake Hiidenvesi, where long transects (about 2000 pixels) and also large lag values were possible, the semivariogram was unbounded. An analysis with cross-correlation yielded the same result.

5. Discussion

The results indicate that under light wind conditions (0–2 $m\,s^{-1}$) the spatial differences of chl-a in a surface water layer can be considerable. In nearly similar weather conditions, the spatial distribution of chl-a can vary from one day to the next. Quite uniform distributions with no clear patches also existed, as demonstrated in Aurlahti bay on 5 August (figure 4(*a*)) and in Pappilanlahti bay on 7 August (figure 5(*c*)). The eddy-like distribution of chl-a in Pappilanlahti bay on 7 August (figure 5(*b*)) is in agreement with the results of Schernewski *et al.* (2000), who concluded that in a small, shallow lake the most pronounced patches were linked to the horizontal circulation eddies. In their study, phytoplankton drifted to the eastern part of the lake and was trapped there by circulation eddies. The flow pattern was due to wind, Coriolis force and morphometry, and pronounced patchiness was only observed under light wind conditions ($<3\,m\,s^{-1}$, Schernewski *et al.* 2000). In stronger winds, the phytoplankton would probably have been more evenly distributed in the studied lakes. According to a modelling study by Webster and Hutchinson (1994) wind speeds exceeding a critical value of 2–3 $m\,s^{-1}$ are required to mix floating

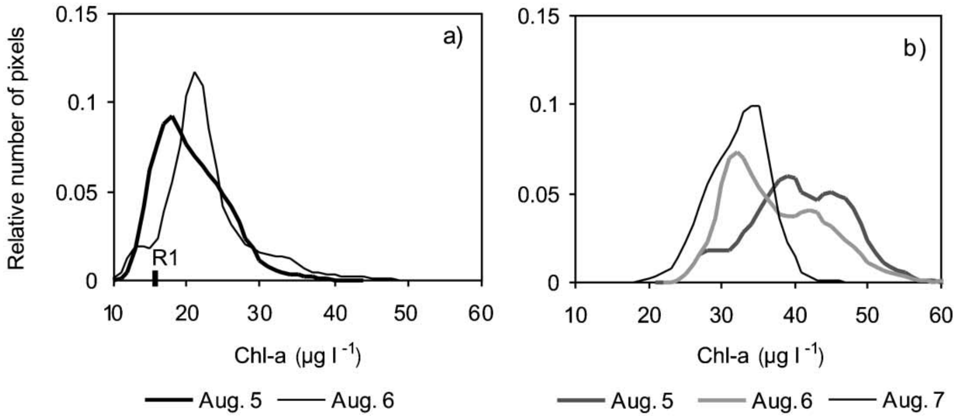

Figure 7. Distribution of chl-a calculated from the chl-a maps of Aurlahti bay (*a*) and Pappilanlahti bay (*b*). In Aurlahti Bay, chl-a at the routine sampling station was 16 μg l^{-1} (indicated by R1) on both days.

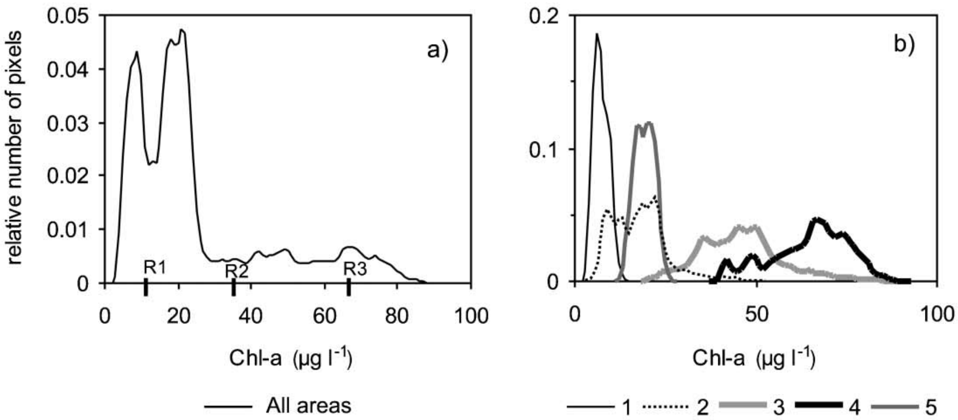

Figure 8. Distribution of chl-a throughout (*a*) and in different areas (*b*) of Lake Hiidenvesi as calculated from the chl-a map. Chl-a at the routine sampling station are indicated by R1 (11 μg l^{-1}), R2 (34 μg l^{-1}) and R3 (66 μg l^{-1}) in (*a*). The location of areas 1–5 is presented in figure 6.

phytoplankton (or colonies) in the water column. This critical value is also supported by observations on the phytoplankton patchiness of a lake dominated by *Aphanizomenon* and *Microcystis* (Horne and Wrigley 1974). Consequently, the spatial distribution of chl-a can be different, depending on whether the wind speed is lower or higher than the critical value.

In Lake Hiidenvesi, the focus was on studying the chl-a distribution between different parts of the lake. The general distribution pattern, an increase in chl-a from west to east and from the centre southwards, is mainly due to the input of external loading into the lake. The main inflowing river, the Vihtijoki, carries nutrient-rich water into the north-eastern part of the lake (figure 1(*b*)). Nutrients may also be released from the bottom sediments in the shallow eastern parts, and this may further increase the nutrient pool available for phytoplankton.

Table 4. Statistical characteristics of the chl-a map of Lake Hiidenvesi on 11 August 1998. The last two columns indicate the statistical characteristics of the observed chl-a at 15 discrete *in situ* sampling stations and AISA-based chl-a at the three routine sampling stations. STD = standard deviation.

	Area 1	Area 2	Area 3	Area 4	Area 5	Areas 1–5	15 stations	3 stations
Number of pixels or stations	470 872	1 324 256	278 027	401 276	536 317	3 010 748	15	3
Area (km^2)	1.88	5.30	1.11	1.61	2.15	12.05	–	–
Mean chl-a ($\mu g\, l^{-1}$)	7.30	17.56	45.94	64.92	19.24	25.19	22.4	37.0
STD	2.05	7.15	11.59	10.58	2.80	19.6	19.7	27.6
Median chl-a ($\mu g\, l^{-1}$)	7	18	45	67	19	19	16	34
Min chl-a ($\mu g\, l^{-1}$)	2	3	18	37	11	2	6.2	11
Max chl-a ($\mu g\, l^{-1}$)	17	53	101	93	28	101	70	66

Table 5. Standard error and observed error of estimated mean chl-a in Lake Hiidenvesi. Observed error was calculated with equation (8). The relative errors indicated in parentheses were obtained by dividing the absolute errors by the true mean chl-a. The true mean chl-a was assumed to be the AISA-based estimation (25.19 $\mu g\,l^{-1}$).

Dataset	Mean chl-a $\mu g\,l^{-1}$	Observed error $\mu g\,l^{-1}$	Standard error $\mu g\,l^{-1}$	Equation used for standard error
AISA data	25.19	–	1.00 (4.0%)	(7)
15 stations	22.41	2.78 (11.0%)	5.08 (20.2%)	(6)
3 routine stations	37.00	11.8 (46.9%)	15.9 (63.3%)	(6)

Since the calculated semivariograms were unbounded, they could not be used to derive the most suitable spatial resolution. This can be due to the fact that the transects (datasets) were not long enough for the analysis. Another reason could be that the semivariograms applied (equation (9)) were not suitable for this type of patchy data. When the semivariogram technique was applied to the digital number measurements (520–600 nm, size $2\,m \times 2\,m$) of an airborne imaging spectrometer (Curran 1988), the optimal spatial resolution for a coastal sea was estimated to be 10 m while in terrestial applications the optimal spatial resolution ranged from 10 to 35 m. According to Curran (1988), semivariograms are less suitable for variables with large spatial differences.

The use of remote sensing data together with discrete water samples clearly improved estimation of the mean chl-a. In Lake Hiidenvesi, the use of AISA data together with 15 discrete water samples yielded a five-fold accuracy improvement (SE for the mean chl-a decreased from 20.2% to 4.0%, table 5), when compared with the use of 15 discrete samples only.

Due to phytoplankton patchiness, routine monitoring programmes may lead to a clear under- or overestimation of the overall phytoplankton concentration in a lake or sub-basin. In Lake Hiidenvesi, the standard error was 63.1% and the observed error 47% (table 5) when the chl-a of three routine monitoring stations was used to estimate mean chl-a. In the two bays of Lake Lohjanjärvi the use of one monitoring station resulted in an under- or overestimation of 29–34% of the overall concentration, compared with the AISA-based estimation (table 3).

The minimum and maximum chl-a in Lake Hiidenvesi were 2 and 101 $\mu g\,l^{-1}$ (AISA data), 6 and 70 $\mu g\,l^{-1}$ (15 *in situ* stations) and 11 and 66 $\mu g\,l^{-1}$ (three routine *in situ* stations). In Lake Hiidenvesi, *in situ* chl-a levels between 5 and 70 $\mu g\,l^{-1}$ were used to determinate the empirical coefficients. The interpreted concentrations outside this range are extrapolations; they are therefore less reliable than other estimations and indicate that chl-a is $<5\,\mu g\,l^{-1}$ or $>70\,\mu g\,l^{-1}$. In the Aurlahti and Pappilanlahti bays the ranges of chl-a on the chl-a map and the algorithm training data were 8–76 $\mu g\,l^{-1}$ and 10–44 $\mu g\,l^{-1}$, respectively. The number of pixels with concentrations lower or higher than those used for training the interpretation algorithm was, however, small, particularly in Lake Hiidenvesi and in Aurlahti bay (figures 7 and 8).

The minimum and maximum chl-a are obtained effectively from the spatially high-resolution remote sensing data. This information can be used to select representative locations for the routine monitoring stations. In Lake Hiidenvesi, for example, a more representative location of the western monitoring station (figure 1(*b*)) could be the most oligotrophic part of the lake in the north-west.

The interpretation of chl-a was here based on a channel ratio, and the coefficients of the empirical algorithm were determined by comparison with *in situ* chl-a. Empirical algorithms are useful as long as the specific inherent optical properties of the water constituents remain the same. At the 662 and 705 nm wavelengths, the most important optical properties are the specific backscattering coefficients of phytoplankton and inorganic suspended solids, and the specific absorption coefficient of phytoplankton. Although no optical measurements were carried out during the 1996 and 1998 surveys it is probable that the optical properties did not differ much within one lake or between the two lakes. The dominant phytoplankton species was the same in different parts of the lakes and the inorganic suspended solids originated from agricultural fields.

The results from Lake Hiidenvesi in August 1996 further confirm that the empirical algorithm applied can be used for chl-a estimation in these lakes. The empirical coefficients of the chl-a algorithm differed only slightly (figure 3) between the lakes and between August 1996 and August 1998 in Lake Hiidenvesi. This indicates that if the dominant phytoplankton species are the same as in this study (*Aphanizomenon spp.*) the same interpretation algorithm could be applied under late summer conditions (August) in these lakes even without *in situ* sampling. The airborne survey carried out in May in Finland resulted in different empirical coefficients for the chl-a algorithm from those found in August (Kallio *et al.* 2001), probably due to differences in specific inherent optical properties.

The remote sensing signal can also be affected by reflection from the lake bottom. In our study, both lakes were quite turbid and Secchi disk transparency ranged between 0.7 and 1.8 m in the surveyed areas. The diffuse attenuation coefficient (K_d) was not measured in the study lakes during the years in question. In August 1997, the $K_{d,\ 660\text{–}710}$ in Aurlahti and Pappilanlahti bays of Lake Lohjanjärvi was 0.6 m^{-1} and 1.3 m^{-1}, respectively. The corresponding attenuation depths ($K_{d,\ 660\text{–}710}{}^{-1}$) were 1.7 and 0.8 m. The effect of the lake bottom is further decreased by the fact that bottom sediments are mostly dark in colour in the surveyed parts of the study lakes. The shallow areas in both lakes are inshore and are usually covered by helophytic macrophytes that normally grow from the shoreline to a depth of 1 m (based on measurements made in Lake Lohjanjärvi in August 2000). The areas with helophytic macrophytes were excluded from the AISA images before the final analyses. It is therefore unlikely that bottom reflection influenced the upwelling radiance measured with the AISA at 662 nm and 705 nm.

Airborne remote sensing provides precise information on the spatial distribution pattern, which is not possible with ground-based techniques. Airborne measurements are particularly useful for phytoplankton process studies and for monitoring a small number of lakes. An entire lake can be surveyed with an airborne imaging spectrometer by making adjacent measurement tracks. The operative monitoring of a large number of lakes by remote sensing can only be based on satellite sensor data. The optimal spatial resolution of a satellite instrument for lake monitoring is probably 30–100 m (IOCCG 2000). Such resolution cannot reveal the small-scale patchiness of phytoplankton, but still gives a more reliable estimation of the overall concentration in a lake than discrete sampling, because an estimation is obtained for pixels that represent an area and not a point. As confirmed by this study, the Envisat MERIS satellite sensor will include channels that make the estimation of chl-a possible in meso-eutrophic lakes. The spatial resolution (pixel size 300 m $\times$ 300 m at best) of MERIS, however, limits its use in small lakes.

Remote sensing can be a valuable tool, particularly in lake-dense regions, such as those in Finland, Sweden, Norway, some parts of Russia and Canada. In these areas the number of lakes is so high that only a small portion of them can be monitored using traditional methods, due to the limited resources available. Moreover, lakes in these countries are often irregularly shaped and include several sub-basins and islands. These factors result in natural variation in water quality that can be further influenced by diffuse and point-source loading. This variation cannot be effectively assessed using monitoring programmes consisting of water sampling at one or a few fixed stations. Best results are obtained by combining remote sensing data with the results of the traditional sampling programmes. Water sampling at the routine stations provides information of the vertical distribution of water quality, reference data (concentrations of the optically active substances, specific inherent optical properties) for the interpretation of water quality from the remote sensing data and concentrations of the variables not possible to monitor by remote sensing.

6. Conclusions

1. The spatial variation in chl-a under light wind conditions (0–2 $m\,s^{-1}$) was considerable in both lakes, and in Lake Lohjanjärvi the distribution pattern changed clearly during two consecutive days.
2. The use of airborne spectrometer data together with discrete sampling data from 15 stations in Lake Lohjanjärvi decreased the relative standard error of the mean chl-a from 20.2% to 4.0%.
3. Routine monitoring based on one or a few sampling stations yielded a 4–63% over- or under-estimation of the mean chl-a compared with the AISA-based estimation.
4. The minimum and maximum chl-a were obtained effectively from the spatially high-resolution remote sensing data. Remote sensing data can be used to identify the most representative locations for the routine sampling stations.

References

Camarero, L., and Catalan, J., 1991, Horizontal heterogeneity of phytoplankton in a small high mountain lake. *Verhandlungen der Internationalen Vereinigung für Theoretische und angewandte Limnologie*, **24**, 1005–1010.

Curran, P. J., 1988, The semivariogram in remote sensing: an introduction. *Remote Sensing of Environment*, **24**, 493–507.

Dekker, A. G., 1993, Detection of optical water quality parameters for eutrophic waters by high resolution remote sensing, PhD Thesis, Vrije Universiteit, Amsterdam.

Dekker, A., Hoogenboom, E., Peters, S., Moen, J. P., Kootwijk, E. J., and Van Rossum, G., 1999, Assessing the quality of inland waters in the Netherlands. *Backscatter*, **10**(1), 15–19.

Dekker, A. G., and Peters, S. W. M., 1993, A TM study of eutrophic lakes in the Netherlands. *International Journal of Remote Sensing*, **14**, 799–821.

Fisher, S. G., 1994, Pattern, process and scale in freshwater ecosystems: some unifying thoughts. In *Aquatic Ecology—Scale, Pattern and Process*, edited by P. S. Giller, A. G. Hildrew and D. G. Raffaelli (London: Blackwell Sciences Ltd), pp. 575–592.

Fraser, R. N., 1998, Hyperspectral remote sensing of turbidity and chlorophyll *a* among Nebraska Sand Hill lakes. *International Journal of Remote Sensing*, **19**, 1579–1589.

Giardino, C., Pepe, M., Brivio, P. A., Ghezzi, P., and Zilioli, E., 2001, Detecting chlorophyll, Secchi disk depth and surface temperature in a sub-alpine lake using Landsat imagery. *The Science of the Total Environment*, **268**, 19–29.

Gitelson, A., 1992, The peak near 700 nm on radiance spectra of algae and water: relationships of its magnitude and position with chlorophyll concentration. *International Journal of Remote Sensing*, **13**, 3367–3373.

Gitelson, A., Garbuzov, G., Szilagyi, F., Mittenzwey, K.-H., Karnieli, K., and Kaiser, A., 1993. Quantitative remote sensing methods for real-time monitoring of inland waters quality. *International Journal of Remote Sensing*, **14**, 1269–1295.

Gitelson, A. A., Yacobi, Y. Z., Schalles, J. F., Ruinquist, D. C., Han, L., Stark, R., and Etzion, D., 2000, Remote estimation of phytoplankton density in productive waters. *Archiv für Hydrobiologie, Advances in Limnology*, **55**, 121–136.

George, D. G., and Malthus, T. J., 2001, Using a compact airborne spectrographic imager to monitor phytoplankton biomass in a series of lakes in north Wales. *The Science of the Total Environment*, **268**, 215–226.

Heege, T., and Fischer, J., 2000, Sun glitter correction in remote sensing imaging spectrometry. *The XV Ocean Optics Conference, 16–20 October 2000* (Falls Church, VA: Office of Naval Research), CD-ROM.

Horne, A. J., and Wrigley, R. C., 1975, The use of remote sensing to detect how wind influences planktonic blue-green algae distribution. *Verhandlungen der Internationale Vereinigung für Theoretische und angewandte Limnologie*, **19**, 784–791.

IOCCG, 1998, Minimum requirements for an operational ocean-colour sensor for the open ocean. Reports of the International Ocean-Colour Coordinating Group, Number 1, Dartmouth, Canada.

IOCCG, 2000, Remote sensing of ocean colour in coastal, and other optically complex, waters. Reports of the International Ocean-Colour Coordinating Group, Number 3, IOCCG, Dartmouth, Canada.

ISO 10260, Water quality—Measurement of biochemical parameters—Spectrometric determination of the chlorophyll-a concentration. International Organization for Standardization.

Jupp, D. L. B., Kirk, J. T. O., and Harris, G. P., 1994, Detection, identification and mapping of cyanobacteria—using remote sensing to measure the optical quality of turbid inland waters. *Australian Journal of Marine and Freshwater Research*, **45**, 801–828.

Kallio, K., Kutser, T., Hannonen, T., Koponen, S., Pulliainen, J., Vepsäläinen, J., and Pyhälahti, T., 2001, Retrieval of water quality from airborne imaging spectrometry of various lake types in different seasons. *The Science of the Total Environment*, **268**, 59–77.

Koponen, S., Pulliainen, J., Servomaa, H., Zhang, Y., Hallikainen, M., Kallio, K., Vepsäläinen, J., Pyhälahti, T., and Hannonen, T., 2001, Analysis on the feasibility of multi-source remote sensing observations for chl-a monitoring in Finnish lakes. *The Science of the Total Environment*, **268**, 95–106.

Lewin, S. A., 1992, The problem of pattern and scale in ecology. *Ecology*, **73**, 1943–1967.

Millie, D. F., Baker, M. C., Tucker, C. S., Vinyard, B. T., and Dionogi, C. P., 1992, High-resolution airborne remote sensing of bloom-forming phytoplankton. *Journal of Phycology*, **28**, 281–290.

Mäkisara, K., Meinander, M., Rantasuo, M., Okkonen, J., Aikio, M., Sipola, K., Pylkkö, P., and Braam, B., 1993, *Airborne Imaging Spectrometer for Applications (AISA), IGARSS Digest* (Tokyo: IGARSS), pp. 479–481.

Mäkisara, K., 1998, *AISA Data User's Guide*, Technical Research Centre of Finland, Research Notes, 1894, 1–54.

Nikulainen, M., Hallikainen, M., Kemppinen, M., Tauriainen, S., Pihlflyckt, J., Taskinen, H., Roschier, M., Valmu, H., and Lauha, M., 1996, Airborne remote sensing platform of the Helsinki University of Technology. *The Second International Airborne Remote Sensing Conference and Exhibition, 24–27 June 1996* (Ann Arbor, NJ: Veridian), pp. 505–514.

O'Reilly, J. E., Maritorena, S., Mitchell, G., Siegel, D., Carder, K., Garver, S., Kahru, M., and McClain, C., 1998, Ocean color chlorophyll algorithm for SeaWiFS. *Journal of Geophysical Research*, **103**, 24 937–24 953.

Östlund, C., Flink, P., Strömbeck, N., Piersson, D., and Lindell, T., 2001, Mapping of the water quality of Lake Erken, Sweden, from imaging spectrometry and Landsat Thematic Mapper. *The Science of the Total Environment*, **268**, 139–154.

Podsetchine, V., and Schernewski, G., 1999, The influence of spatial wind inhomogenity on flow patterns in a small lake. *Water Research*, **33**, 3348–3356.

Pulliainen, J., Kallio, K., Eloheimo, K., Koponen, S., Servomaa, H., Hannonen, T., Tauriainen, S., and Hallikainen, M., 2001, A semi-operative approach to water quality retrieval from remote sensing data. *The Science of the Total Environment*, **268**, 79–93.

Rast, M., Bėzy, J., and Bruzzi, S., 1999, The ESA Medium Resolution Imaging Spectrometer MERIS—a review of the instrument and its mission. *International Journal of Remote Sensing*, **20**, 1681–1702.

Reynolds, C. S., 1994. The role of fluid motion in the dynamics of phytoplankton in lakes and rivers. In *Aquatic Ecology—Scale, Pattern and Process*, edited by P.S. Giller, A.G. Hildrew and D.G. Raffaelli (London: Blackwell Sciences Ltd), pp. 141–187.

Schernewski, G., Podsetchine, V., Asshoff, M., Garbe-Schönberg, D., and Huttula, T., 2000, Spatial ecological structures in littoral zones and small lakes: examples and future prospects of flow models as research tools. *Archiv für Hydrobiologie, Advances in Limnology*, **55**, 227–241.

Schalles, J. F., Gitelson, A. A., Yacobi, Y. Z., and Kroenke, A. E., 1998, Estimation of chlorophyll *a* from time series measurements of high spectral resolution reflectance in a eutrophic lake. *Journal of Phycology*, **34**, 383–390.

Stauffer, R. E., 1982, Wind stress effects on chlorophyll distribution in stratified eutrophic lakes. *Limnology and Oceanography*, **27**, 66–74.

Tallberg, P., Horppila, J., Väisänen, A., and Nurminen, L., 1999, Seasonal succession of phytoplankton and zooplankton along a trophic gradient in a eutrophic lake—implications for food web management. *Hydrobiologia*, **412**, 81–94.

Van Stokkom, H. T. C., Stokman, G. N. M., and Hovenier, J. W., 1993, Quantitative use of passive optical remote sensing over coastal and inland water bodies. *International Journal of Remote Sensing*, **14**, 541–563.

Vos, R., and Rijkeboer, M., 2000, Monitoring of algal blooms in Case 2 waters with SeaWIFS. *The XV Ocean Optics Conference, 16–20 October 2000* (Falls Church, VA: Office of Naval Research), CD-ROM.

Verhagen, J. H. G., 1994, Modelling phytoplankton patchiness under the influence of wind-driven currents in lakes. *Limnology and Oceanography*, **39**, 1551–1565.

Webster, I. T., and Hutchinson, P. A., 1994, Effect of wind on the distribution of phytoplankton cells in lakes revisited. *Limnology and Oceanography*, **39**, 365–373.

Wrigley, R. C., and Horne, A. J., 1974, Remote sensing and lake eutrophication. *Nature*, **250**, 214–215.

Yacobi, Y. Z., Gitelson, A., and Mayo, M., 1995, Remote sensing of chlorophyll in Lake Kinneret using high-spectral-resolution radiometer and Landsat TM: spectral features of reflectance and algorithm development. *Journal of Plankton Research*, **17**, 2155–2173.